REGULAR PAPER

Dynamic cell culture device using electroactive polymer actuators with composite electrodes to transfer in-plane mechanical strain to cells

Dong-Uk Kim[1] · Seungjin Lee[1] · Seung-Hwan Chang[1]

Abstract

Living tissues in the body receive various types of stimuli, including mechanical strain, pressure, and varied chemical environments. In contrast, conventional cell cultures are processed under in vitro conditions, which are not similar to the actual body's environment. To precisely simulate the human body environment, a dynamic cell culture device capable of applying mechanical stimulation to cells is needed. In this study, an acrylic dielectric elastomer electroactive polymer (EAP), is introduced as a driving component for a dynamic cell culture device with a simple structure. The device is composed of separated upper and lower modules with a driving film at the center, By assembling these components, the electrodes on the surface of the driving film are isolated but still connected by columns that can transfer the deformation of the driving apparatus to the culture membrane. The culturing performance of cells according to the mechanical stimuli was experimentally investigated and compared. Tensile strain was found to provide the highest improvement in cell development rate, reaching up to 32.3%. These results highlight the utility of EAPs for compact and biocompatible dynamic cell culture device design.

Keywords Dielectric elastomer · Cell culture device · PDMS (polydimethylsiloxane) · Composite electrodes

1 Introduction

The cell cytoskeleton plays many important roles in cellular function, in addition to providing structural rigidity. The cytoskeleton is composed of microfilaments that enable cell migration and differentiation, intermediate filaments that withstand mechanical stress and support organelles, and microtubules involved in cell motility, cell differentiation, and intracellular transport. These components play an essential role in determining cell morphology, motility, and mechanical properties. The cytoskeleton is also linked to the extracellular matrix (ECM) by focal adhesion, which mechanically connects the ECM, the cell membrane, and the nucleus to each other.

The mechanism of dynamic cell cultures are still not clear, and requires further study [1]. Various attempts to effectively transfer physical stimuli to cells have been made, including flowing culture medium or applying a compressive or tensile load. Culturing cells in these dynamic environments is known to produce different results from static cell cultures. Rashidi et al. [2] applied fluid shear stress to hepatocyte-like cell (HLC) through the Quasi-Vivo® system (Kirkstall Limited, UK) and found it improved the metabolic capacity and somatic cell phenotype of HLC. Dhein et al. [3] used a FlexCell stretch system (FlexCell International Corp., USA) to apply periodic mechanical stretches to cardiomyocytes, allowing the cardiomyocytes to be grown in an inclined direction approximately 11°–25° to the stretch axis within 24 h. Kaspar et al. [4] devised an experimental method to give the cells a uniform elongation with a four-point bending device and performed a two-day test for 30 min a day. The result confirmed excellent cell proliferation, increasing by 10–48% compared to a static cell culture. Lam et al. [5] showed that myoblasts (C2C12) rapidly realign within 24 h by periodically applying compressive

✉ Seung-Hwan Chang
phigs4@cau.ac.kr

1   School of Mechanical Engineering, Chung-Ang University, 221 Heukseok-Dong, Dongjak-Gu, Seoul 156-756, Republic of Korea

force to a polydimethylsiloxane (PDMS) dish with wavy microfeatures.

Jung et al. [6] designed a dynamic cell culture apparatus delivering 1% strain to cells cultured on a silicon film using an EAP actuator made of an OMMT-containing silicone film. Davis et al. [7] demonstrated that shape memory polymers that can deliver mechanical stimuli to cells while maintaining high cell viability and adhesion can be used to control cell alignment in cell cultures. In addition, Brown [8] compared the main characteristics of various culture devices for the delivery of mechanical stimuli to cell and tissue cultures. Three signaling systems regulate cellular activity: chemical, electrical, and mechanical [9]. Mechanical loads can be further classified into tensile, compressive, and shear forces. There are significant effects on the cell proliferation rate, substrate formation rate, and alignment direction when cells are periodically placed under tension for a short time.

Experimental results show that aortic endothelial cells are reoriented with minimal matrix deformation in response to periodic uniaxial tension [10]. Winter et al. [11] imposed cyclic uniaxial tension for 60 min on bone marrow stromal cells from rat femurs. The intermittently stimulated cells, with alternating 15-min stimulation/rest loading sets, were more affected than the continuously stimulated cells. These osteoblast-like cells appear to respond better to intermittent deformation than to continuous deformation.

Dynamic cell culture devices require large scale power sources, usually motors, to simulate the body environment and induce cell deformation. A sterile environment in a CO_2 incubator is also generally required to create an environment suitable for cell growth. Motors not only take up space in narrow incubators, but also are difficult to sterilize, which can lead to contamination of cultured cells.

In this study, we report a small dynamic cell culture device using electroactive polymers (EAPs) as a driving apparatus, which deforms according to the applied voltage. Dielectric elastomers, a widely used class of EAP, exhibit responsive behavior similar to muscles [12–14], and can realize various mechanical behaviors in response to applied voltages with relatively fast reaction speed [15, 16], making it useful as a small actuator for dynamic cell culturing. The EAP actuator can transfer tensile or compressive stress (or strain) to the cell according to the magnitude and frequency of applied voltage. Because the cell culture device can be connected to the outside power source by a simple electrical connection, this approach is space-efficient with no risk of contamination. Fibroblasts extracted from human lungs were cultivated using a dynamic cell culture device described above to test its performance.

2 Experimental

2.1 Materials and structures of the cell culture device

The cell culture device designed in this study consists entirely of PDMS except for the driving apparatus. PDMS is a dielectric elastomer and biocompatible polymer with no cytotoxicity. It also has excellent insulation performance, elasticity, and moldability, making it is useful in many research fields, such as sensor and actuator fabrication, in addition to biotechnology [17–22]. The driving apparatus is composed of a dielectric elastomer film with a flexible electrode pasted on the surface. EAP actuators can be fabricated in various ways depending on the material and driving method [23–26]. Because high frequency is not required to transmit stimulus to the cell, acrylic elastomer (VHB 4910, 3 M, USA) was used to induce high deformation through the actuator [27]. The dielectric constant of the acrylic elastomer used in this study is 5 F/m, the Young's modulus is 0.5 MPa, the breakdown strength is 100 MV/m [28], and the energy density is 3.2 J cm^{-3} [29]. This material is suitable as a large deformable actuator because of its high force density.

To supply a stable driving voltage, a flexible electrode with robust electrical resistance under deformation is required. Conductive carbon grease (M.G. Chemicals, Canada) has a relatively low electrical resistance (114 Ω cm) and high electrical conductivity and was used without inhibiting the deformation of the dielectric elastomer. This mixture of conductive carbon black and grease is commonly used for EAP electrodes.

2.2 Fabrication process of modules

The cell culture device is composed of an upper and lower PDMS module. The upper module has an area for the cell culture, and the lower module contains the EAP thin film, which acts as the driving apparatus. The thin film is abutted against columns running through both the upper and lower modules. A 3D printer was used to fabricate molds for the PDMS modules. The outer dimensions of the printed structure were similar to existing cell culture dishes with a diameter of 55 mm, and a culture area 25 mm in diameter. Because inverted microscopes are generally used for observing cells in culture, the bottom of the upper module should be transparent [30]. Therefore, the mold for the upper module was made of acrylic, and the culture area was mirror-surfaced to facilitate cell observation and cell culture. Grid patterns were added to the mold to help identify the position of the cells under a microscope. The

upper portions of the two molds are shaped like a spoke to allow air bubbles to escape during vacuum decompression, while also allowing the modules to be mechanically coupled when they are assembled. The PDMS and the curing agent were mixed at a mass ratio of 10:1, and gas bubbles were removed by vacuum depressurization. First, the lower mold was placed in a petri dish, and the bubble-free PDMS mixed solution was added. After assembling the upper mold, secondary bubble removal was performed by applying vacuum. After curing for 12 h or more in an oven at 40 °C, the PDMS module was separated from the mold.

2.3 Fabrication of EAP actuator (driving film)

EAP actuators made of 1 mm thick acrylic elastomer (VHB4910) films were pre-stretched by 600% for high driving displacement. To hold the pre-stretched dielectric elastomer in place, a ring-shaped fixing frame made of polycarbonate was used. The frame had an outer diameter of 32 mm, an inner diameter of 25 mm, and was 1.5 mm thick. A flat stretching device (Fig. 1), capable of simultaneously stretching in eight directions, was designed to accomplish a uniform and stable pre-strain (600%).

To prepare the driving apparatus, the film was cut along the outer circumference of the frame while maintaining the deformation state by fixing the frame on both sides of the stretched acrylic film. A thin layer of conductive carbon grease was coated on both sides of the film to construct an electrode. Carbon grease is easy to handle and maintains large deformation compared to other electrode materials because the conductive carbon powder is mixed in a grease-based viscous matrix [31]. As shown in Fig. 2, in order for the developed cell culture apparatus to be driven, the upper and lower modules must be firmly fastened, and electric power must be effectively supplied to the electrode located on both sides of the driving film. Therefore, a thin, flexible, and conductive PDMS film was used to connect the power supply to the electrode, without altering the shape of the fastener.

To make the conductive PDMS composite electrode film, PDMS, and a curing agent were mixed at a 10:1 mass ratio, conductive carbon black powder was mixed with this PDMS solution at a 17:3 mass ratio, and bubbles were removed by

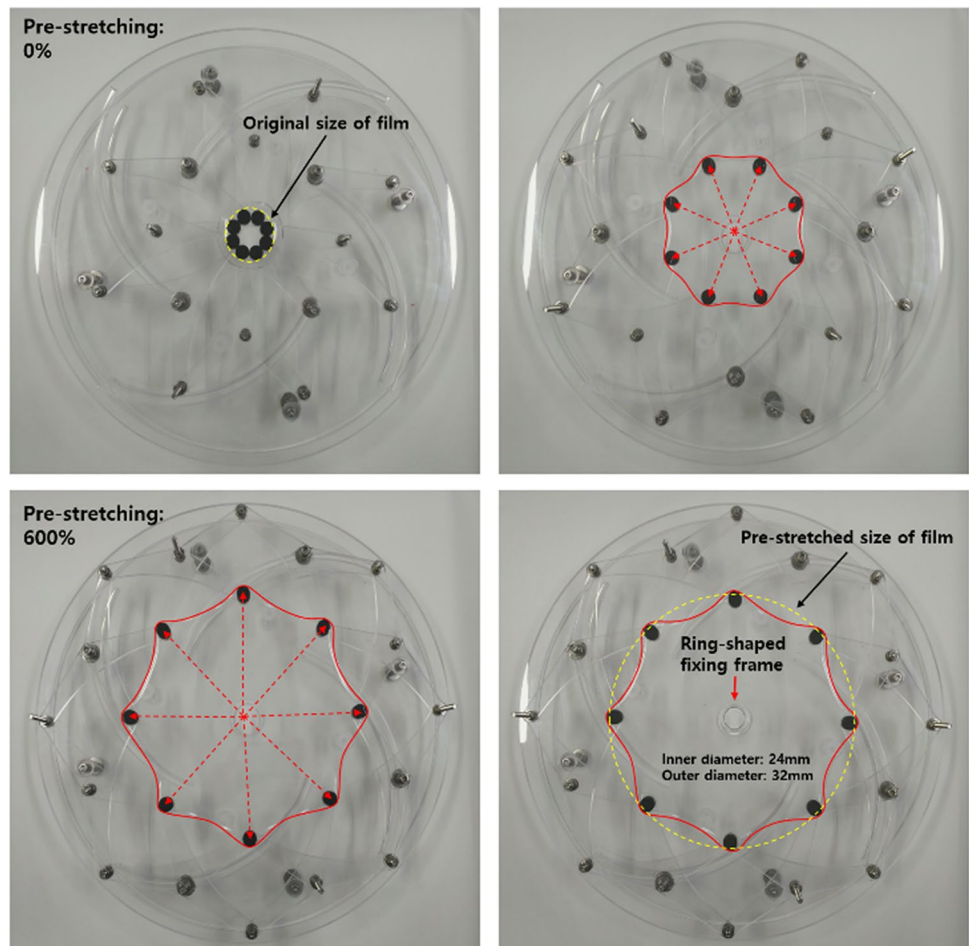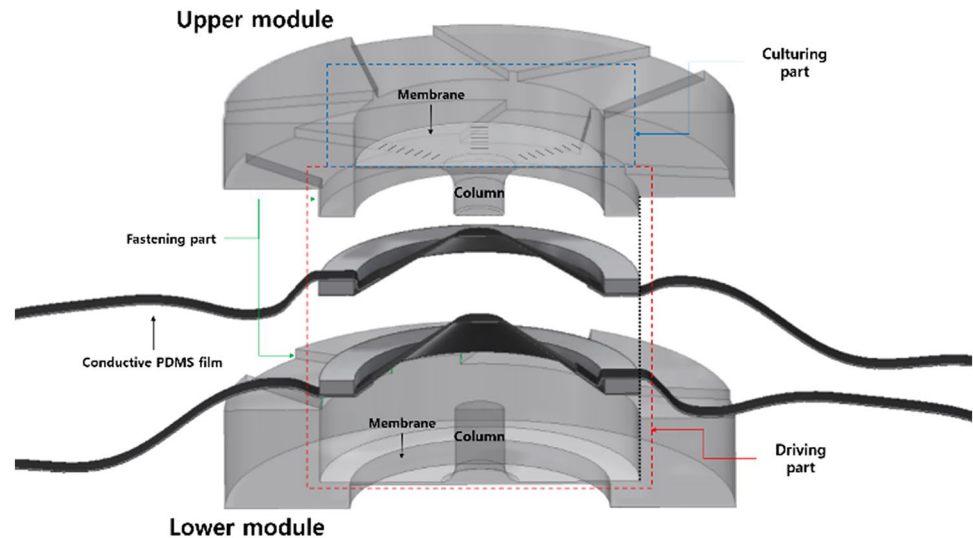Fig. 1 Pre-stretching device and fabrication process

applying vacuum for 1 h. The PDMS solution containing carbon black was uniformly applied on a PET film with a thickness of 200 μm, and cured at 80 °C for 1 h to produce a flexible electrode. The resistivity of the film is rather high (37.5 kΩ cm), but EAP is a dielectric elastomer, which acts as a capacitor, and the resistance of the electrode only affects the charge rate of the electrodes when a voltage is applied. This does not affect the deformation of the EAP. As shown in the cross-sectional view of Fig. 2, two conductive PDMS driving films are connected to the carbon grease electrodes on the top and bottom surfaces of the acrylic film to serve as wires.

The designed cell culture device is divided into a culture area and a driving apparatus, as shown in Fig. 2. The bottom of the culture area is a membrane which is deformed by the driving film through a column in the upper module. The cells are cultured in a space completely independent of the driving apparatus. The driving apparatus is composed of the columns and membranes of both modules and the dielectric elastomer (circular driving film). When the upper and lower modules are completely tightened in the axial direction, the upper and lower columns are brought into contact with the driving film between them, and the driving film is fastened.

When electric power is applied to the driving film, it deforms, inducing axial movement of the contacted columns. This produces mechanical deformation to the culture area in the upper membrane. The upper module is easily replaceable to facilitate cell seeding for cultivation, and the top membrane of the upper module is able to directly incubate cells. In addition, the upper module membrane spatially separates and insulates the driving apparatus from the culture unit, thereby preventing damage to the cells by the current. The shape of the bottom of the upper module enables fastening to the lower module, and the height of the upper module is matched to the column height (5.2 mm) to

minimize focusing problems caused by membrane deformation during microscope observation.

The two mating columns move in the axial direction according to the level of activation in the circumferential direction to fix the rim of the circular driving film, which can be easily replaced when damaged. The column of the lower module provides additional pre-tension to the circular driving film when the modules are engaged, of the circular acrylic driving film under electric fields. As shown in Fig. 2, the lower module is grooved in the crucible, also transferring the elastic force of the driving film to the membrane.

Varying elastic forces in the membrane control the deformation of the device, as the axial load applied to the columns is disrupted from equilibrium by the driving film due to the applied voltage (see Fig. 3a). When no voltage is applied, the elastic forces of the driving film and the upper module membrane are stronger than that of the lower module membrane, therefore the upper module membrane is kept in a planar state. When a voltage is applied, the driving film expands, and the elastic force relaxes, causing the columns to rise from the elastic force of the lower module membrane. This results in deformation of the upper module membrane. To amplify the deformation, two layers of driving film (see Fig. 2) were used in this study.

2.4 Calculation of the driving deformation

To evaluate the exact amount of strain applied to the cells according to the applied voltage, the vertical displacement of the columns were measured. The deformation occurring in the culture area (upper membrane) was estimated using an analytic approach and was verified by finite element analysis (FEA). Movement of the driving apparatus was photographed by attaching a visual marker to the center of the culture area. Resulting images were processed using

Fig. 3 Driving apparatus of the device: **a** driving mechanism of the cell culture device. **b** Schematic of the driving apparatus for calculating deflection
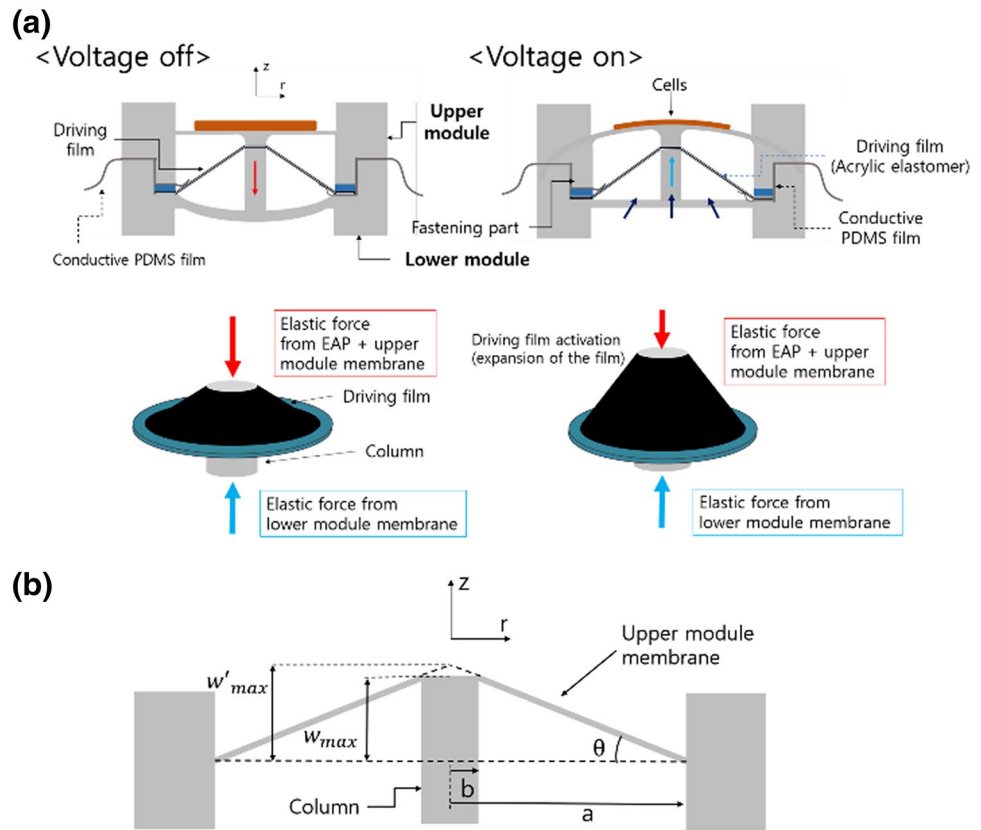
MATLAB to measure the vertical displacement. By using a voltage amplifier (Trek-623B, USA) and a function generator (Agilent 33210A, USA), a sine wave voltage signal with an amplitude of 0.5–4.8 kV (peak voltage $\pm$ 2.4 kV) and frequency of 1 Hz was applied to the EAP driving film. The amount of radial deformation in the driving film gradually increased, due to displacement occurring in the opposite direction of gravity at the center of the circular film. Cell growth is greatly affected by radial strain from the circular culture dish (the membrane of the upper module). The strain distribution occurring on the surface of the culture dish was calculated as described below.

The membrane of the culture dish is assumed to be a thin circular plate, and a concentrated central force is applied under the clamped edge condition at the rim [32]. The flexural rigidity (D) of the plate is defined by Eq. 1 where the membrane thickness (t) is 0.5 mm. The Young's modulus (E) and Poisson's ratio (ν) of PDMS are 2.66 MPa and 0.5, respectively [33].

$$D = \frac{Et^3}{12(1-v^2)} \tag{1}$$

The deflection with respect to the radius of the membrane can be calculated by Eq. 2. Here, P is the concentrated force acting on the center, r is the radius of the membrane, and a

is the maximum in-plane radius (radius of culture area, see Fig. 3b) of the membrane.

The 4 mm-diameter column transfers the force from the driving film, which affects the actual deflection of the membrane, and needs to be considered in this calculation.

$$w(r) = \frac{P}{16\pi D}\left(2r^2 ln\frac{r}{a} + a^2 - r^2\right) \tag{2}$$

Therefore, the pseudo-deflection $\left(w'_{max}\right)$, which has the same radial slope as the actual membrane of the upper module (Fig. 3b), was introduced. By using this relationship and Eq. 4 the axial load P was estimated.

$$\frac{w_{max}}{a-b} = \frac{w'_{max}}{a} \tag{3}$$

$$w'_{max} = w_0 = \frac{Pa^2}{16\pi D} \tag{4}$$

As a result, the deflection with respect to the radius can then be expressed by the following equation:

$$w(r) = \begin{cases} w_{max}, 0 \leq r < b \\ \frac{P}{16\pi D}\left(2r^2 ln\frac{r}{a} + a^2 - r^2\right), b \leq r \leq a \end{cases} \tag{5}$$

The radial strain of the circular plate is defined by Eq. 6, and the double derivative of Eq. 5 with respect to *r* becomes Eq. 7. The radial strain is finally defined by Eq. 8. Where *z* is distance from the centerline of the plate, for radial strain to occur at the surface, the value of *z* must be at least 0.25 mm.

$$\varepsilon_r = -z\frac{d^2w}{dr^2} \tag{6}$$

$$\frac{d^2w}{dr^2} = \begin{cases} 0, 0 \leq r < b \\ \frac{P\left(ln\frac{r}{a}\right)+P}{4\pi D}, b \leq r \leq a \end{cases} \tag{7}$$

$$\varepsilon_r(r) = \begin{cases} 0, 0 \leq r < b \\ -zP\left(\frac{ln\frac{r}{a}+1}{4\pi D}\right), b \leq r \leq a \end{cases} \tag{8}$$

The strain distribution calculation from this analytic approach was verified by FEA using a commercial finite element code, ABAQUS. For the finite element modeling, the membrane and column of the culture area were considered, and the edge of the PDMS membrane was fixed. Linear analysis was performed under the condition that the maximum displacement of the center of the driving apparatus in the z-direction due to column movement was 0.33 mm. Linear hexahedral elements (C3D8R) were used for the analysis, and the approximate element size was set to 0.125 mm. The number of elements and nodes were 244,626 and 219,362, respectively.

2.5 Cell culture experiments

The cell culture process is illustrated in Fig. 4. For the upper module, where the cells are directly cultured, sterilization was performed for 2 min using oxygen plasma equipment to increase sterilization. During this process, oxygen plasma treatment enhances cell adhesion on the surface of PDMS. When the PDMS surface deforms the strain can be transferred to the cells thru the focal adhesion. Bonding spots called 'focal adhesion' are formed between cells and PDMS surface during cell culture. This focal adhesion connects solid surface, adhesive protein and actin filament so the cells can fix or move themselves to the surface. Sterilization of the lower module, where the driving apparatus is assembled, was first performed using an autoclave, followed by alcohol and UV sterilization after the driving film had been mounted. MRC-5 fibroblasts (ATCC CCL-171) derived from human lungs were used for the culture. The upper module was seeded with 1 ml of cell suspension containing 100,000 cells, and the culture medium was Dulbecco's modified Eagle's medium (DMEM, Gibco®, Thermo Fisher Scientific, Waltham, MA, USA) supplemented with 10% fetal bovine serum (FBS, Gibco®, USA) and 1% antibiotic–antimycotic

solution (Gibco®, Thermo Fisher Scientific, Waltham, Mass., USA).

Prior to the stimulation application experiment, the cells were cultured in an incubator overnight at 37 °C, 95% humidity, and 5% carbon dioxide concentration to confirm cell adhesion. The culture medium was replaced and the cells were cultured for another 24 h to increase the number of cells. In the driving experiment, a function generator (Agilent 33210A, USA) was connected to a voltage amplifier (Trek-623B, USA), and an AC sine wave was applied to the module with a peak of ± 1.5 kV, which induced 0.33 mm maximum vertical displacement of the column. To estimate the loading effects on cell development, cell states were investigated immediately following and 24 h after stimulation. Cells were stained by replacing the culture medium with 1 ml of fresh medium containing two drops of NucBlue® Live ReadyProbes ™ Reagent (NucBlue®, Thermo Fisher Scientific, Waltham, MA, USA) to confirm the exact number of cells.

The cell thickness has the range of 0.5 ~ 1.5 μm [34]. To compare the number of cells under each condition only the cells attached on the surface of the driving part which can be identified by the focusing state of a microscope were counted. Cell counting was carried out by using ImageJ (NIH, US) which counts the stained cell nuclei but the spheroid was excluded in the cell counting.

3 Results and discussion

3.1 Driving displacement of the cell culture device

Figure 5a shows the displacement generated by applying a 1 Hz AC voltage with a sine waveform. When the peak voltage is ± 2.5 kV, the Z-axis displacement is 0.67 mm. The load, P, of 4.635×10^{-3} N can be obtained by substituting 0.33 mm in w_{max} (when the applied voltage is ± 1.5 kV) in Eqs. 3 and 4. By inserting the values of a (12.5 mm), b (2 mm) and D (3.694×10^{-2} N•mm) into Eq. 8, the radial strain of the membrane can be found, as shown in Fig. 6a.

To precisely investigate the exact strain distribution, FEA was performed. Because of the actual shape of the column attached to the membrane and its flexibility (hyperelasticity) the strain distribution near the column is little bit different from the calculation result (Eq. (8)), but the trend of gradually decrease of the radial strain was similar to the calculated result. The overall strain distribution was found to range from − 0.3 to 0.4% when maximum displacement of the column occurred, as shown in Fig. 6. The radial strain of the membrane at r = 6.4 mm is estimated to be zero. As a result, the generated strains are tensile when the radius is less than 6.4 mm and compressive when the radius exceeds this value (see Fig. 6).

Fig. 4 Cell culture process
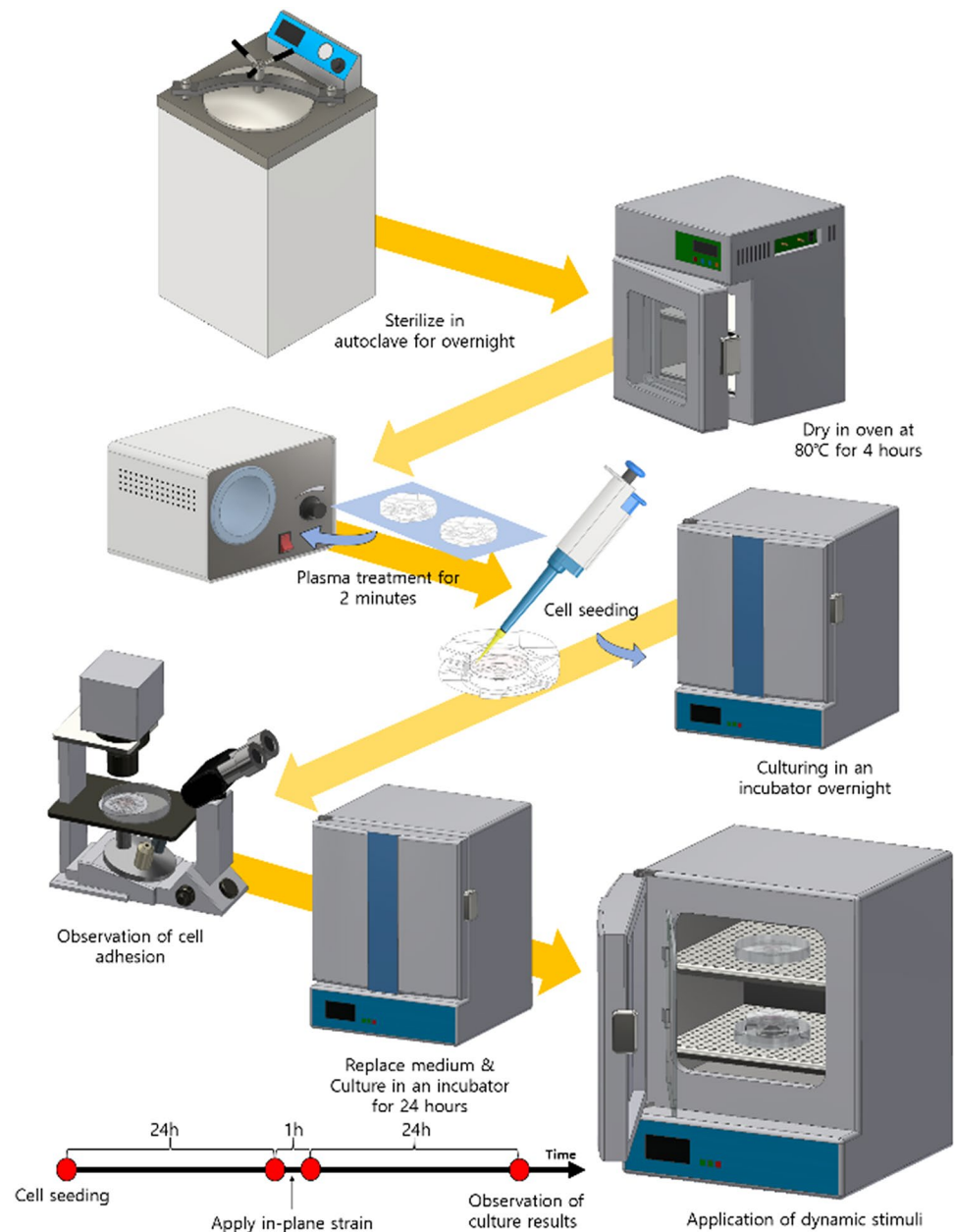
Due to the dielectric elastomer having the same structure as the parallel plate capacitor, charge and discharge occur quickly when an alternating voltage is applied, and deformation of the EAP occurs in the same pattern as the absolute value of the voltage. The relationship between the voltage signal and the resulting radial strain is shown in Fig. 5b, where two maxima can be found in a 1 Hz cycle. Note that the membrane is deformation free at neutral voltage neutral.

3.2 Cell culture experiment

The results of the cell culture are shown in Fig. 7. A control group with no mechanical strain and the same culture duration was maintained to investigate the effect of radial strain on cell development. After 1 day, the development rate of control group was below 1%, while the development rate of dynamic cell was 4.37% when a 1 Hz radial mechanical strain was applied (Fig. 4). The development rate changed based on the level of strain, as shown in Fig. 7b–f. The edge of the driving film had the highest compressive strain (-0.362%), which produced the highest development rate, 10.7% (Fig. 7b). At r = 9 mm, the strain and development rate was found to be -0.294% and 7.99%, respectively (Fig. 7c).

Measurements near the center ($r = 6$ mm) displayed -0.071% of strain, and the cell development rate

Fig. 5 Radial strain distribution of the culture area: **a** radial strain distribution from the analytic calculation, **b** FEA result of strain distribution and the corresponding cell differentiation rate
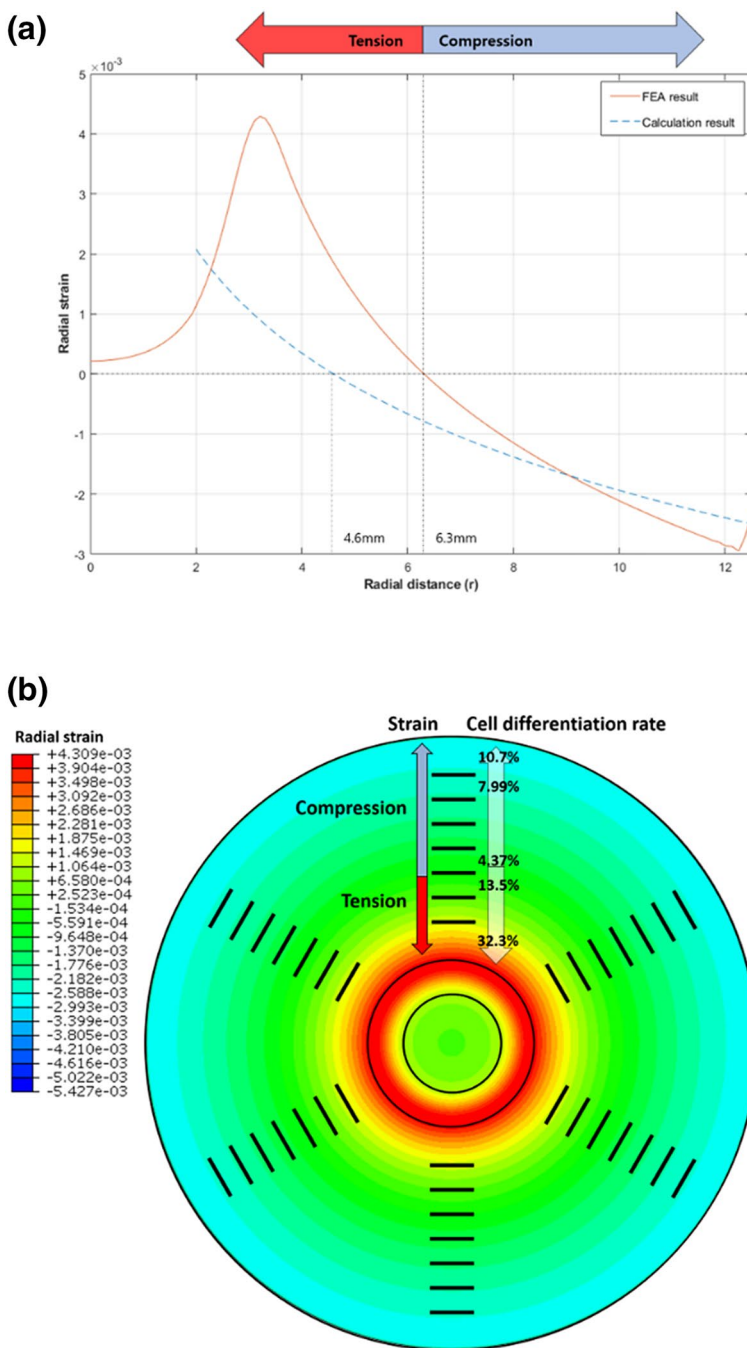

decreased to 4.37%, as shown in Fig. 7d. When $r = 5$ mm, 0.044% of tensile strain occurred and the cell development rate drastically increased to 13.5% (Fig. 7e). Although the absolute magnitudes of strain were similar at $r = 5$ and 6 mm ($- 0.071\%$ vs. 0.044%), the cell growth results were quite different, indicating a cell preference for tensile strain. The driving film produced the highest cell development rate (32.3%) at the location of maximum tensile strain (0.596%) near the column ($r = 2$, Fig. 7f).

From these experimental results, we find that when dynamic stimulus is imposed, viable cells develop at a rate at least four times greater than static cultures. Interestingly, the cell development rate is affected not only by the magnitude of the stimulus, but also the type of stimulus (compressive vs. tensile).

Because this dynamic cell culture device uses high voltage, electric fields generated around the cells may affect development, array, and transporting of cells, as previously

Fig. 6 Driving displacement under electric loading condition: **a** moving distance of column when AC voltage applied. **b** The generated strain distribution of the culture part under when AC voltage applied
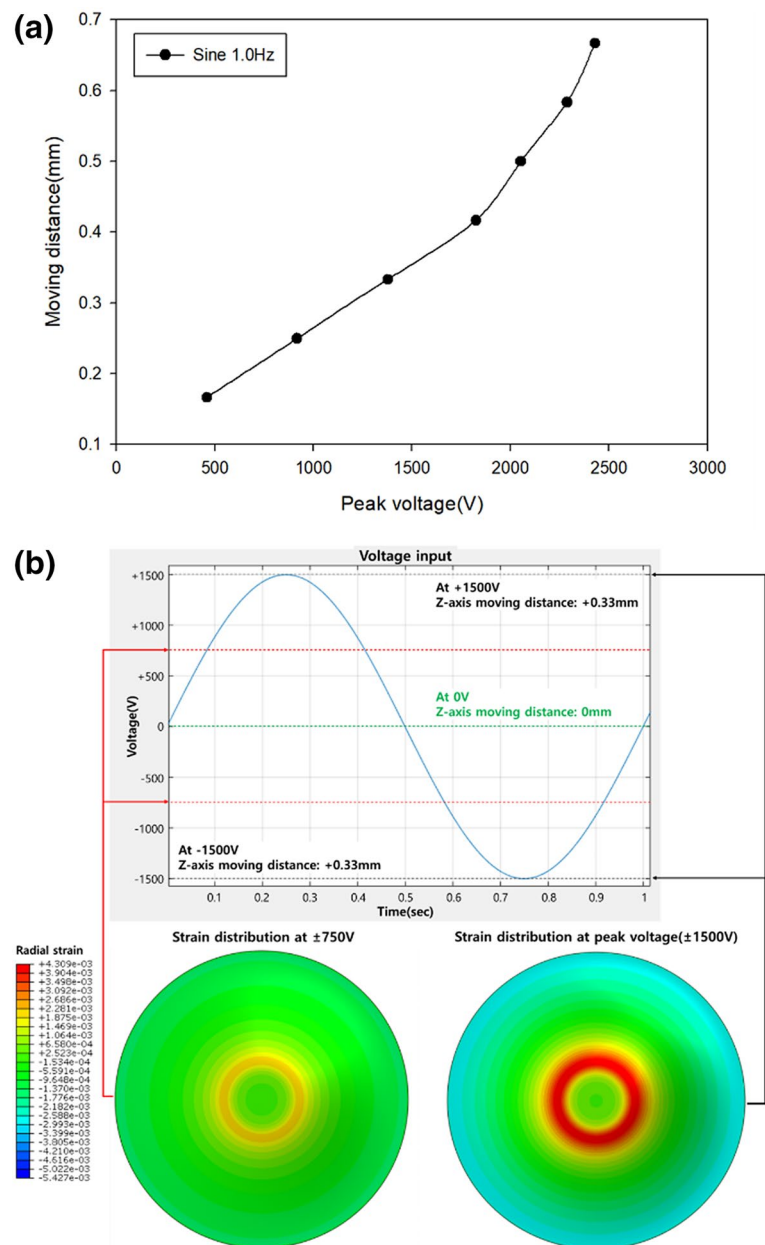
described [35, 36]. However, because the dielectric elastomers in our device have the same shape as a parallel plate capacitor, the electric fields generated by electrodes that propagate outward cancel each other and become zero.

The improvement in cell viability in our dynamic cell culture apparatus is not influenced by an increased electric field. There are several similar studies on dynamic cell culturing using different devices. Winter et al. [11] invented a device that provides tensile force to cells but used electric motor as the driving unit, making it too large and difficult to sterilize. In contrast, our device is easy to sterilize and can simultaneously apply various stimuli to cells.

Based on these results, we find that the dynamic cell culture device designed in this study can effectively deliver stimulus to cells through a simpler process than previous methods. In addition, the operation requires connecting only a pair of wires inside the incubator, greatly reducing contamination risk and improving space efficiency. Because the upper module acts as a dish, it is possible to apply stimulation to existing cell culture experiments, enabling further stimulation application experiments without needing to develop new culture methods.

4 Conclusions

A cell culture device made of a biocompatible material (PDMS) was designed with separated modules and a dielectric elastomer actuator. The upper module membrane, which
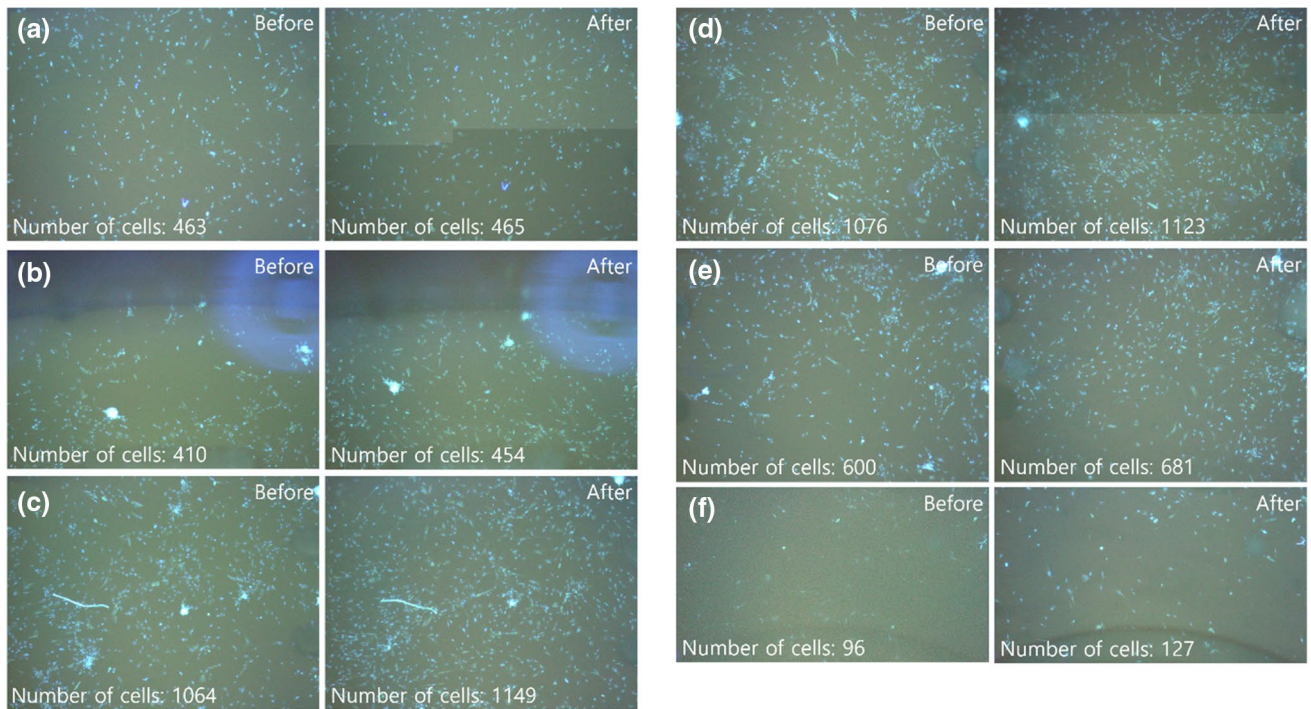
Fig. 7 Results of 24-h cell culture: **a** control group [strain: 0% (static state), cell differentiation rate: 0.432%]. Experimental groups of **b** compressive strain: 0.362%, cell differentiation rate: 10.7%. **c** Compressive strain: 0.294%, cell differentiation rate: 7.99%. **d** Compressive strain: 0.071%, cell differentiation rate: 4.37%. **e** Tensile strain: 0.0437%, cell differentiation rate: 13.5%. **f** Tensile strain: 0.596%, cell differentiation rate: 32.3%

serves as a culture plate, has a mirror surface and enables accurate observation of cells. The device can be miniaturized and simplified in structure, and is operated through a wire connection to reduce the risk of contamination, allowing for operation in existing incubators.

Owing to the mechanism by which the circular driving film is deformed, the culturing area (upper membrane) experiences a progressively increasing radial deformation from edge to center. Using this property, both radial compressive and tensile strains can be applied to cells being cultured. The magnitude of strain can be manipulated by adjusting the voltage applied to the driving film.

To confirm the feasibility of using this dynamic stimulus to improve cell culturing, human lung fibroblast was used for culture experiments. By regulating the voltage applied to the driving film, a 1 Hz mechanical stimulation was imposed on the cells in culture, generating periodic displacement for 1 h.

The cell development was observed 24 h after the end of the stimulus application to evaluate the cell culture performance. When maximum tensile strain (0.596%) of the culturing cells occurred, the number of cells increased by 32.3%. Cells that experienced maximum compressive strain (−0.362%) increased by 10.7%. The control group with no dynamic stimulus had an increase of less than 1%. Our results show that cell development is improved through

mechanical strain, and tensile deformation produces greater effects than compression.

The use of a PDMS EAP actuator avoids several technical problems that have limited previous device architectures, such as poor biocompatibility, electric breakdown, contamination, and a variety of stimuli. The upper module membrane spatially separates and insulates the driving film from the culture unit, thereby preventing contamination and damage to the cells by electrical current. This also helps to avoid breakdown of the dielectric elastomer under high driving voltage conditions.

The actuator made of dielectric elastomers usually have high deformation during driving condition, therefore flexible electrodes which provide stable electric conductivity are essential. In this study, carbon grease was used for this purpose but it has relatively short service life [31]. For a long-term service more efficient flexible electrodes need to be tried and it is known that CNT [37], AgNWs [38], eutectic GaInSn alloy [39] are promising materials for fabricating flexible electrodes. As proved in Kaspar's experiments [4] dynamic cell culture is effective even the stimulating period is short relative to the conventional static cell culture. However, it was also proved that the period and cycle of the applied stimuli also affected the cell development according to Winter's experimental study [11].

However, the developed culturing device can only provide in-plane mechanical stimulus to the attached cells, which is a major limitation of this approach. To develop more efficient cell culturing, various additional mechanical stimuli should be applied to the cells [40, 41]. Devices with multiple modes of operation should be developed because favorable culturing conditions may change according to the type of cells. Moreover, loading period and cycle should also be considered to find the most appropriate condition for cell culture. The development of a three-dimensional cell culture device using an electroactive polymer actuator with a corresponding extracellular matrix is a good candidate to address these needs, and is the focus of our future work.

Compliance with ethical standards

Conflict of interest On behalf of all authors, the corresponding author states that there is no conflict of interest.

References

1. Bao G, Suresh S (2003) Cell and molecular mechanics of biological materials. Nat Mater 2(11):715–725. https://doi.org/10.1038/nmat1001
2. Rashidi H, Alhaque S, Szkolnicka D, Flint O, Hay DC (2016) Fluid shear stress modulation of hepatocyte-like cell function. Arch Toxicol 90(7):1757–1761. https://doi.org/10.1007/s00204-016-1689-8
3. Dhein S, Schreiber A, Steinbach S, Apel D, Salameh A, Schlegel F et al (2014) Mechanical control of cell biology. Effects of cyclic mechanical stretch on cardiomyocyte cellular organization. Prog Biophys Mol Biol 115(2–3):93–102. https://doi.org/10.1016/j.pbiomolbio.2014.06.006
4. Kaspar D, Seidl W, Neidlinger-Wilke C, Ignatius A, Claes L (2000) Dynamic cell stretching increases human osteoblast proliferation and CICP synthesis but decreases osteocalcin synthesis and alkaline phosphatase activity. J Biomech 33(1):45–51. https://doi.org/10.1016/s0021-9290(99)00171-2
5. Lam MT, Clem WC, Takayama S (2008) Reversible on-demand cell alignment using reconfigurable microtopography. Biomaterials 29(11):1705–1712. https://doi.org/10.1016/j.biomaterials.2007.12.010
6. Jung KC, Jeon GJ, Bae JH, Chang SH (2015) Flexible cell culture device made of membrane-type silicone composites for simulating human body. Compos Struct 134:36–43. https://doi.org/10.1016/j.compstruct.2015.08.054
7. Davis KA, Burke KA, Mather PT, Henderson JH (2011) Dynamic cell behavior on shape memory polymer substrates. Biomaterials 32(9):2285–2293. https://doi.org/10.1016/j.biomaterials.2010.12.006
8. Brown TD (2000) Techniques for mechanical stimulation of cells in vitro: a review. J Biomech 33(1):3–14. https://doi.org/10.1016/S0021-9290(99)00177-3
9. Yang C, Zhang XH, Guo YC, Meng FJ, Sachs F, Guo J (2015) Mechanical dynamics in live cells and fluorescence-based force/tension sensors. Biochim Biophys Acta Mol Cell Res 1853(8):1889–1904. https://doi.org/10.1016/j.bbamcr.2015.05.001
10. Wang JHC, Goldschmidt-Clermont P, Wille J, Yin FCP (2001) Specificity of endothelial cell reorientation in response to cyclic mechanical stretching. J Biomech 34(12):1563–1572. https://doi.org/10.1016/S0021-9290(01)00150-6
11. Winter LC, Walboomers XF, Bumgardner JD, Jansen JA (2003) Intermittent versus continuous stretching effects on osteoblast-like cells in vitro. Journal of Biomedical Materials Research Part A 67a(4):1269–1275. https://doi.org/10.1002/jbm.a.20028
12. Romasanta LJ, Lopez-Manchado MA, Verdejo R (2015) Increasing the performance of dielectric elastomer actuators: a review from the materials perspective. Prog Polym Sci 51:188–211. https://doi.org/10.1016/j.progpolymsci.2015.08.002
13. Brochu P, Pei QB (2010) Advances in dielectric elastomers for actuators and artificial muscles. Macromol Rapid Commun 31(1):10–36. https://doi.org/10.1002/marc.200900425
14. Jiang L, Betts A, Kennedy D, Jerrams S (2015) Investigation into the electromechanical properties of dielectric elastomers subjected to pre-stressing. Mater Sci Eng C Mater Biol Appl 49:754–760. https://doi.org/10.1016/j.msec.2015.01.070
15. Ariano P, Accardo D, Lombardi M, Bocchini S, Draghi L, De Nardo L et al (2015) Polymeric materials as artificial muscles: an overview. J Appl Biomater Funct Mater 13(1):1–9. https://doi.org/10.5301/jabfm.5000184
16. Belanger MC, Marois Y (2001) Hemocompatibility, biocompatibility, inflammatory and in vivo studies of primary reference materials low-density polyethylene and polydimethylsiloxane: a review. J Biomed Mater Res 58(5):467–477. https://doi.org/10.1002/jbm.1043
17. Lee JH, Ji WY (2003) Electrical and mechanical properties of silicone rubber for high voltage insulation. In: Proceedings of the 7th international conference on properties and applications of dielectric materials, vols 1–3, pp 591–594
18. Ye XD, Liu HZ, Ding YC, Li HS, Lu BH (2009) Research on the cast molding process for high quality PDMS molds. Microelectron Eng 86(3):310–313. https://doi.org/10.1016/j.mee.2008.10.011
19. Kim SH, Lee S, Ahn D, Park JY (2019) PDMS double casting method enabled by plasma treatment and alcohol passivation. Sens Actuators B Chem 293:115–121. https://doi.org/10.1016/j.snb.2019.04.145
20. Bae JH, Chang SH (2015) Characterization of an electroactive polymer (PVDF-TrFE) film-type sensor for health monitoring of composite structures. Compos Struct 131:1090–1098. https://doi.org/10.1016/j.compstruct.2015.06.075
21. Choi YW, Jang S, Chun MS, Kim SM, Choi M (2018) Efficient microfluidic power generator based on interaction between DI water and hydrophobic-channel surface. Int J Precis Eng Manuf Green Technol 5(2):255–260. https://doi.org/10.1007/s40684-018-0026-5
22. Kwon JY, Park HW, Park YB, Kim N (2017) Potentials of additive manufacturing with smart materials for chemical biomarkers in wearable applications. Int J Precis Eng Manuf Green Technol 4(3):335–347. https://doi.org/10.1007/s40684-017-0039-5
23. Jung KC, Chang SH (2019) Performance evaluation of smart grid fabrics comprising carbon dry fabrics and PVDF ribbon sensors for structural health monitoring. Compos Part B Eng 163:690–701. https://doi.org/10.1016/j.compositesb.2019.01.050

24. Bae JH, Chang SH (2019) PVDF-based ferroelectric polymers and dielectric elastomers for sensor and actuator applications: a review. Funct Compos Struct 1(1):012003. https://doi.org/10.1088/2631-6331/ab0f48

25. Tajeddini V, Muliana A (2017) Deformations of flexible and foldable electro-active composite structures. Compos Struct 160:280–291. https://doi.org/10.1016/j.compstruct.2016.09.069

26. Jayaramudu T, Li Y, Ko HU, Shishir MDIR, Kim J (2016) Poly(acrylic acid)-poly(vinyl alcohol) hydrogels for reconfigurable lens actuators. Int J Precis Eng Manuf Green Technol 3(4):375–379. https://doi.org/10.1007/s40684-016-0047-x

27. Michel S, Zhang XQQ, Wissler M, Lowe C, Kovacs G (2010) A comparison between silicone and acrylic elastomers as dielectric materials in electroactive polymer actuators. Polym Int 59(3):391–399. https://doi.org/10.1002/pi.2751

28. Sommer-Larsen P, Larsen AL (2004) Materials for dielectric elastomer actuators. Smart Struct Mater 2004 Electroactive Polym Actuators Devices (Eapad) 5385:68–77. https://doi.org/10.1117/12.539500

29. Yuan X, Changgeng S, Yan G, Zhenghong Z (2016) Application review of dielectric electroactive polymers (DEAPs) and piezoelectric materials for vibration energy harvesting. J Phys Conf Ser 744:012077. https://doi.org/10.1088/1742-6596/744/1/012077

30. Kim DU, Chang SH (2019) Design of an actuator using electro-active polymer (EAP) actuator with composite electrodes. Compos Res 32(5):211–215. https://doi.org/10.7234/composres.2019.32.5.211

31. Rosset S, Shea HR (2013) Flexible and stretchable electrodes for dielectric elastomer actuators. Appl Phys A Mater Sci Process 110(2):281–307. https://doi.org/10.1007/s00339-012-7402-8

32. Bhaskar K, Retd TK (2014) Analysis of circular plates. In: Analysis of circular plates, pp 69–88

33. Wang Z (2011) Polydimethylsiloxane mechanical properties measured by macroscopic compression and nanoindentation techniques. University of South Florida, Tampa

34. Lin CH, Wang CK, Chen YA, Peng CC, Liao WH, Tung YC (2016) Measurement of in-plane elasticity of live cell layers using a pressure sensor embedded microfluidic device. Sci Rep. https://doi.org/10.1038/srep36425

35. Li L, El-Hayek YH, Liu BS, Chen YH, Gomez E, Wu XH et al (2008) Direct-current electrical field guides neuronal stem/progenitor cell migration. Stem Cells 26(8):2193–2200. https://doi.org/10.1634/stemcells.2007-1022

36. Yao L, Shanley L, Mccaig C, Zhao M (2008) Small applied electric fields guide migration of hippocampal neurons. J Cell Physiol 216(2):527–535. https://doi.org/10.1002/jcp.21431

37. Yuan W, Hu LB, Yu ZB, Lam TL, Biggs J, Ha SM et al (2008) Fault-tolerant dielectric elastomer actuators using single-walled carbon nanotube electrodes. Adv Mater 20(3):621. https://doi.org/10.1002/adma.200701018

38. Lee YR, Kwon H, Lee DH, Lee BY (2017) Highly flexible and transparent dielectric elastomer actuators using silver nanowire and carbon nanotube hybrid electrodes. Soft Matter 13(37):6390–6395. https://doi.org/10.1039/c7sm01329a

39. Liu Y, Gao M, Mei SF, Han YT, Liu J (2013) Ultra-compliant liquid metal electrodes with in-plane self-healing capability for dielectric elastomer actuators. Appl Phys Lett. doi 10(1063/1):4817977

40. He YL, Macarak EJ, Korostoff JM, Howard PS (2004) Compression and tension: differential effects on matrix accumulation by periodontal ligament fibroblasts in vitro. Connect Tissue Res 45(1):28–39. https://doi.org/10.1080/03008200490278124

41. Win Z, Buksa JM, Steucke KE, Luxton GWG, Barocas VH, Alford PW (2017) Cellular microbiaxial stretching to measure a single-cell strain energy density function. J Biomech Eng Trans ASME. doi 10(1115/1):4036440

Dong-Uk Kim M.S. candidate in the Department of Mechanical Engineering from Chung-Ang University. His research interests include electroactive polymer and designing dynamic cell culture device.
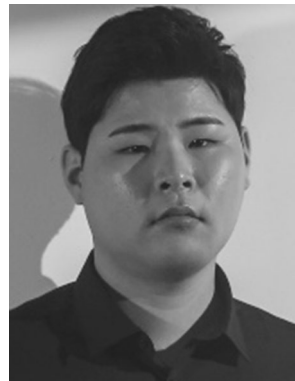
Seungjin Lee Ph.D. candidate in the Department of Mechanical Engineering from Chung-Ang University. His research interests include organ-on-a-chip and microfluidics.

Seung-Hwan Chang Professor in School of Mechanical Engineering, Chung-Ang University, Seoul. His research is focused on functional materials ranging from electroactive polymers (EAPs), to design of biologic composite prostheses for bone healing and to self-powered wearable fabric sensors and actuators.